3D Modelling of Building Pounding Including Diaphragm Flexibility

G.L. Cole, R.P. Dhakal & A.J. Carr
University of Canterbury, New Zealand

D.K. Bull
University of Canterbury, New Zealand
Holmes Consulting Group Ltd, New Zealand

15 WCEE
LISBOA 2012

SUMMARY:
The role of diaphragm flexibility is investigated for 3D modelling of building pounding. Two existing three storey buildings are modelled undergoing impact for various building separations with and without diaphragm flexibility. The resulting damage is classified as either local or global building damage. Local and global damage is found to respond differently to changes in building separation. Global damage generally reduces with increasing building separation, however local damage is largely insensitive. Differences between the categories are also found when predictions are made using the less accurate rigid diaphragm assumption. Global damage appears to be reasonably predicted when multiple analyses are used to find an average building response. However, local damage cannot be predicted in this way.

Keywords: pounding, 3D analysis, diaphragm rigidity, impact, local damage

1. INTRODUCTION

Building pounding describes the collision of adjacent buildings due to earthquake ground motions. Such collision occurs when the buildings' relative movement exceeds their initial separation. When collision occurs it results in a large magnitude but short duration contact force in each building, which results in momentum transfer between the buildings. Pounding is known to be a highly complex phenomenon (Anagnostopoulos and Spiliopoulos 1992; ULIEGE 2007; Lopez-Garcia and Soong 2009), which requires detailed modelling for accurate predictions of building performance. This need for accuracy has driven previous researchers to consider the three dimensional response of buildings due to pounding (Papadrakakais et al. 1996; Mouzakis and Papadrakakis 2004; Jankowski 2009; Jankowski 2012). However, to date these modelling techniques have not explicitly considered the role of diaphragm flexibility on these predictions.

The authors have previously investigated the role of diaphragm flexibility in two dimensional building analyses, and found that diaphragm flexibility can significantly affect building pounding response under certain conditions (Cole et al. 2011). When building floors are modelled as being perfectly rigid, a source of energy loss (due to axial oscillation) is eliminated from the model. In certain situations, this energy loss can have a significant effect on the predicted response of the colliding buildings. The role of diaphragm flexibility is investigated here for the three dimensional response of a single building configuration. These analyses are performed assuming all impacted floors cause collision with the floors of neighbouring buildings (floor/floor collision).

2. LOCAL AND GLOBAL BUILDING DAMAGE

Predicted building pounding damage can be categorised as either local damage or global damage. *Local damage* describes the damage that is caused by the direct application of the contact force. Examples of local damage from floor/floor collision include spalling at the point of impact, and

damage to the impacted floor. *Global damage* is a consequence of the momentum transfer that occurs during collision. After a collision, a building may have more (or less) momentum in its floor. This change in dynamic properties can result in increased interstorey drifts over the remainder of the ground motion. These greater drifts cause greater member demands.

In most previous research, attention has been entirely focused on global building damage. This has been primarily because the collision force could not be accurately calculated. However, previous work by the authors has shown that collision force can be calculated when each colliding floor is modelled with distributed mass and flexibility (Cole et al. 2011). Local and global building damage are considered separately in the following sections.

3. ADOPTED BUILDING MODEL

3.1 Main Features of the Analysis

Building modelling was performed using *Ruaumoko3D* (Carr 2007), a non-linear time history programme developed at the University of Canterbury. Uniform modal damping (Wilson and Penzien 1972) was adopted in all modelling. This is because the more commonly adopted Rayleigh damping causes high levels of damping in the higher frequency modes. In these analyses, the higher frequency modes are important because they are excited during collision. Pounding analyses are also sensitive to the adopted integration time step. In these analyses, the time step is set at 5×10^{-5} seconds. This was determined by reducing the time step until the equations of motion conserved the total model energy over the duration of the ground motion. At a time step of 10^{-4} seconds, an acceptable energy loss of <1% was recorded. Building beams and columns are modelled using Modified Takeda law with $\alpha = 0.5$ and $\beta = 0$ as recommended by Dong (2003), with the post elastic stiffness set at 1% of the initial stiffness.

3.2 Building Selection

Two 1960's three-storey buildings were selected for modelling. These buildings are both currently in use in Wellington, New Zealand. The buildings can be characterised as buildings with favourable geometry (such as low total height, no major building irregularities) but primitive earthquake restraint systems (masonry infilled panels). The buildings were selected because they represent a common pounding risk observed in New Zealand towns and cities. In reality, the two modelled buildings are not actually located adjacent to one another, so the results presented here represent a strictly theoretical risk.

While the existing buildings selected for modelling have infilled panels, the panels are assumed to contribute negligible stiffness to each building's response. This assumption is made because buildings of this era typically cast the concrete columns prior to building the infill masonry panels. This decision resulted in gaps between the masonry and the surrounding column, which isolates the masonry panels. The presented models are thus assumed to act as reinforced concrete frame structures. It would be possible to develop much more detailed panel models which allow the activation of masonry panels once the specified gap is closed; however such an approach would require lengthy development time that is not currently available to the authors.

The adopted building configuration is presented in Figure 3.1. Soil-structure interaction is also modelled, but omitted from the figure for clarity. Note that while some adjacent floors are not at exactly the same height, a completely horizontal collision force is assumed. This is because the differences in floor height are less than the depth of the perimeter beams of these walls.

Soil structure interaction is simulated using the fundamental lumped parameter model (Wolf 1994). This model simulates the movement of a rigid disk on an elastic halfspace using viscous dampers, elastic springs and additional masses. Soil properties were obtained through from bore logs of one of

the selected buildings, and conversations with practising geotechnical engineers from Beca, Carter, Hollings and Ferner Ltd, who are familiar with Wellington soils (Table 3.1).
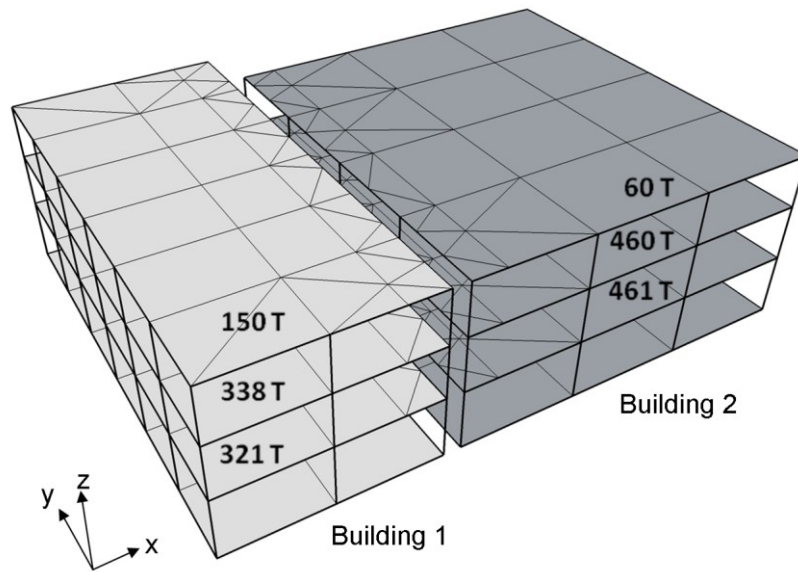

Figure 3.1 Modelled building configuration

Table 3.1 Adopted soil properties

Property	Value	Calculation method	Source
Shear stiffness G_{max}	175 MPa	$G_{max} = 325N_{60}^{0.68}$ [In Kips] *	Bore log
Soil density ρ	1937 kg/m³	-	Beca
Poisson's Ratio ν	0.3	-	Beca
Shear wave velocity c_s	290 m/s	$c_s = \sqrt{\dfrac{G_{max}}{\rho}}$	-

* Formula obtained from Kramer (1996)

3.3 Ground Motion Records

Three excitation records were used in the pounding analyses; El Centro (Imperial Valley, 1940), Tabas (Iran, 1978), and La Union (Mexico, 1985). These particular records are adopted because they are considered to possess similar characteristics to a major rupture of the Wellington fault. The records have been scaled according to NZS1170.5:2004. This scaling requires selection of a soil class. The soil class (type C) was selected based upon the soil type of Te Aro, a central Wellington suburb with many buildings with pounding potential. The ground motions are scaled for the 1/25 year event. This corresponds to a 'service level' motion in the current New Zealand standard (NZS1170.5 2004) and is roughly equivalent to the 'ultimate' design criteria when the buildings were constructed in the 1960s (Fenwick and MacRae 2009). In the early 1960s, buildings were constructed using the 1935 New Zealand building code, which used the working stress design method. Fenwick and MacRae (2009) converted the working stress method to an equivalent limit state formulation to allow comparison to current New Zealand codes. They found that the 1935 code produced an equivalent horizontal seismic shear of $0.104W_t$, where W_t is the seismic weight of the considered structure. The 1/25 year horizontal seismic shear in the current New Zealand standard is $0.1W_t$ for Wellington.

3.4 3D Contact Element

Collision between all floors was modelled using elastic Kelvin elements including contact friction effects (Figure 3.2). The Kelvin element simulates contact using a large spring stiffness that is only activated when the specified building separation is exceeded. Friction forces can be created during this collision when the buildings attempt to slide relative to each other (Figure 3.2, Right). In the presented analyses the coefficient of friction is set at $\mu = 0.4$, as recommended by Pallett et al. (2002) for hardened concrete-to-concrete interaction.

Twelve contact elements were used at each floor level, which were located at the external corners of each diaphragm element along the contact interface (refer Figure 3.1). The contact element stiffness (k_x) was calculated using a similar philosophy to that adopted in previous 2D modelling (Cole et al. 2011). This was done by setting the contact element stiffness equal to the smaller axial stiffness of the colliding floors at the considered nodes (i.e. the smaller of the axial diaphragm stiffness at Node A and Node B in Figure 3.2, Left). These stiffnesses were calculated by taking tributary width measurements as shown in Figure 3.3. When beams were aligned parallel to the direction of the anticipated contact force, and were located at the considered node, their stiffness was added to that calculated in the diaphragm.
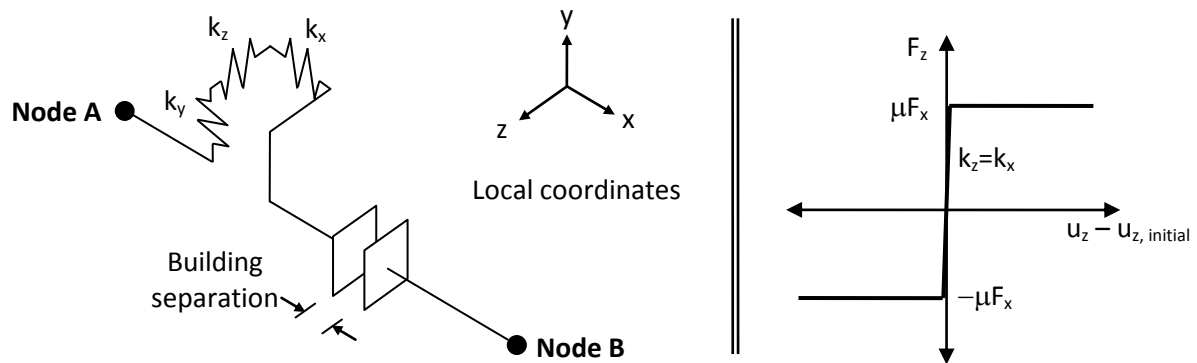

Figure 3.2 Adopted contact element. Left: Element layout. Right: Adopted friction model for the local z axis
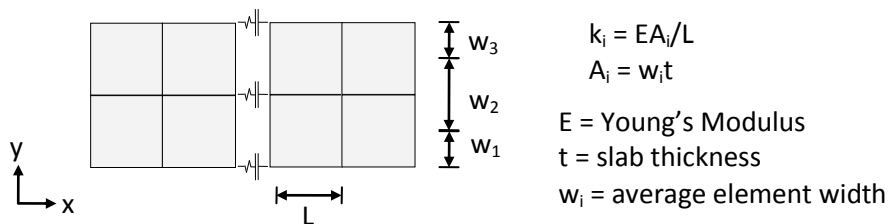

Figure 3.3 Plan view of two colliding floors showing example calculation of axial element stiffness. This process is an intermediate step in determining contact element stiffness

4. EFFECTS OF INCREASING BUILDING SEPARATION

4.1 Global Damage

This section investigates the increase in global building demands caused by building collision. Analyses were run for each ground motion with varying building separations (building separations of 0, 5, 10, 15, 25, 35, 40 and 45 mm were analysed). Figure 4.1 presents the amplification of interstorey shears due to pounding in Building 2. Building separation values (shown on the horizontal axis) are normalised by the minimum building separation required to prevent pounding. These values have been

individually calculated for each ground motion. A normalised separation of 1.0 indicates the buildings are just sufficiently separated to prevent pounding for the analysed ground motion. This point therefore represents the performance of the considered building without any collision.
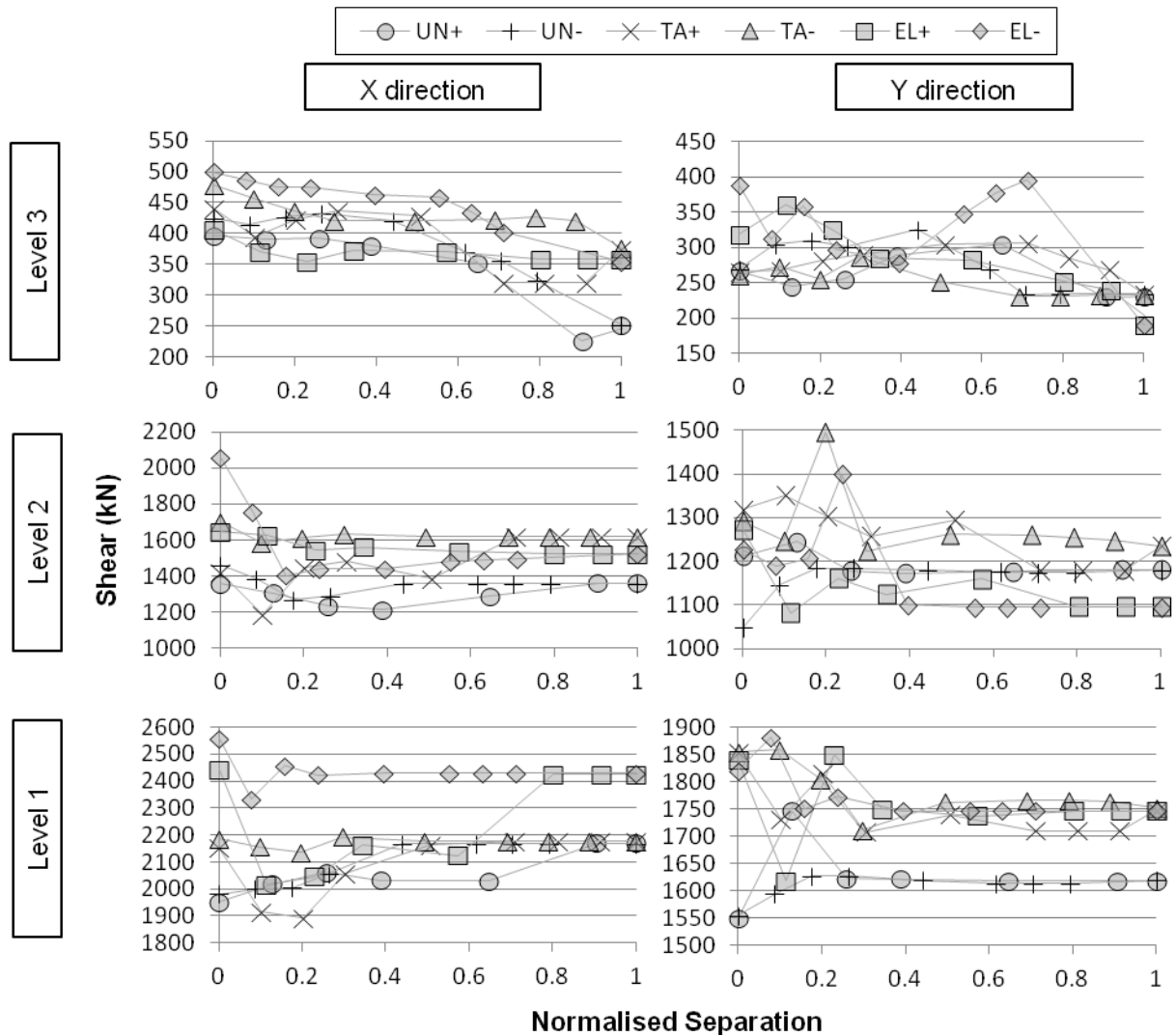

Figure 4.1 Building 2 shear amplification due to pounding

Interpretation of interstorey shear amplifications is difficult since many elements yielded during the performed analyses. Building 2's shear amplifications are presented here since no column yielding occurred in the building during the no collision (NC) analyses. During the pounding analyses yielding did occur in the Level 3 columns; however in all cases except one, this was limited to the four corner columns. This yielding has therefore made little difference to the total interstorey shear.

Greater percentage shear amplifications occurred in the higher stories, however all level's responses change significantly in at least one pounding analysis. At roof level, shear demands reach up to twice that of the NC demand. At Level 2, shears are amplified by up to a maximum of 38%. However, these amplifications are unlikely to trigger any failure because the amplified shear is still less than the base shear in the NC case, which usually dictates the column shear capacity (the column shear capacity will be significantly higher than the base shear if capacity design principles are followed). As expected, these amplifications very rarely caused column yielding. The shear at Level 1 is also Building 2's base shear, which is frequently used as a measure of expected building damage. However, when pounding occurs, amplification of the base shear differs from the amplifications of other floors. The base shear is amplified by 18% in the worst case. This indicates that base shear amplification should not be used as

the only measure of building response amplification due to pounding. Amplifications in the Y direction are approximately equal to that in the X direction at all levels. These results demonstrate that pounding is able to both amplify and deamplify building demands (compared to building demands without pounding), depending on the specific model configuration. Increasing the separation of the buildings generally reduces these shear amplifications.

Figure 4.2 presents the maximum recorded member curvature ductilities that correspond to building movement in the X direction (see Figure 3.1). Building 1 is more sensitive to pounding effects in comparison to Building 2. This result is likely to be due to the greater overall mass of Building 2. Building 2's ductilities are reduced at all separations greater than 0 mm, while approximately half of Building 1's actions have been reduced by pounding. This again shows how global damage has an inconsistent affect on building response. As observed in the shear results, ductility values generally converge to NC results with increasing building separation. For example, for a normalised separation of 0.5 or greater, pounding induced demands differ from the NC records by less than 28%. However, at 0 separation these differences can be more than 100%. In the worst case, the beam curvature ductility demand in Building 1 increases to 9, which is easily sustained by a reasonably detailed plastic hinge. Nevertheless, given that the buildings used in the analysis represented old New Zealand buildings in which the modern ductile detailing may not have been followed; a ductility demand of 9 may test the beams' deformation capacities.
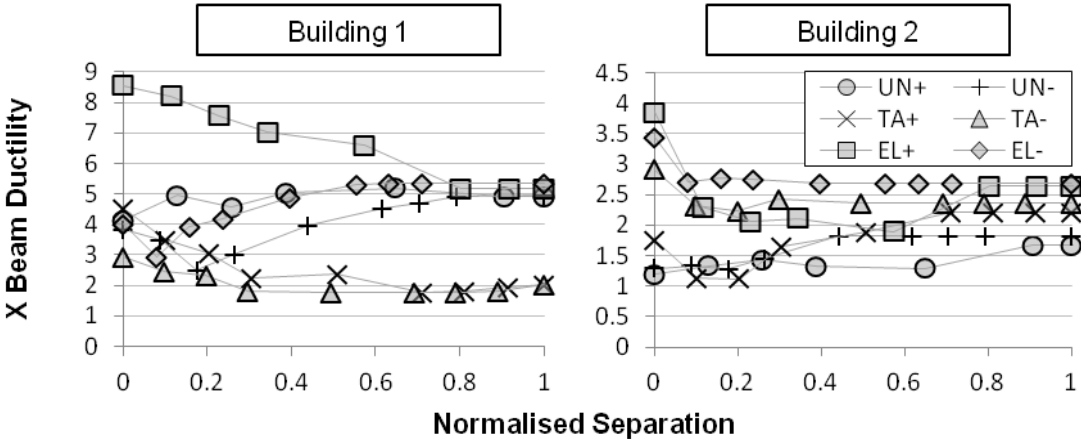

Figure 4.2 Beam ductility due to movement in the X direction

4.2 Local Damage

Local damage measures respond differently to global damage measures. The maximum axial contact forces are presented for each record in Figure 4.3. Level 2's contact forces are considerably larger than Level 3's forces and Level 1 also records larger forces than Level 3 at 0 mm separation. This is due to the much larger floor masses at these levels (refer Figure 3.1). Contact force reduces with increasing separation at Level 1, but at other levels the forces remain reasonably constant. This insensitivity to building separation is an important distinction from that observed in the global damage results. In general terms, global damage reduces roughly proportionally with separation, while local damage is insensitive to separation. This means that buildings with a separation of 80% (say) of that required to prevent pounding may still experience major contact forces, while suffering little global damage.
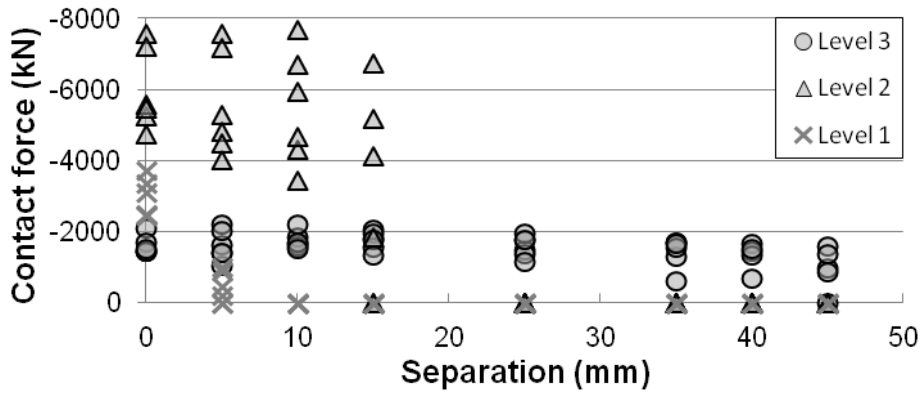
Figure 4.3 Axial contact force results with increasing building separation

5. EFFECTS OF FLOOR RIGIDITY

5.1 Global Damage Changes Due to Floor Rigidity

Interstorey shear amplifications are presented in Figure 5.1. These results are found by dividing the rigid diaphragm results (called *3DRigid*) by the results obtained for the same analysis with flexible diaphragms (called *3DModel*). In the following figures, data is identified by building separation (in mm). The mean and mean ± one standard deviation of the data is indicated with a black line and two grey lines, respectively. Shear forces are generally overestimated by the rigid diaphragm models. Building 1's X direction shear amplifications are observed to be suppressed due to the extensive yielding in the building's columns. Y axis Shears are affected more than the X axis shears. This is attributed to the horizontal friction forces during contact and is discussed in the next section.
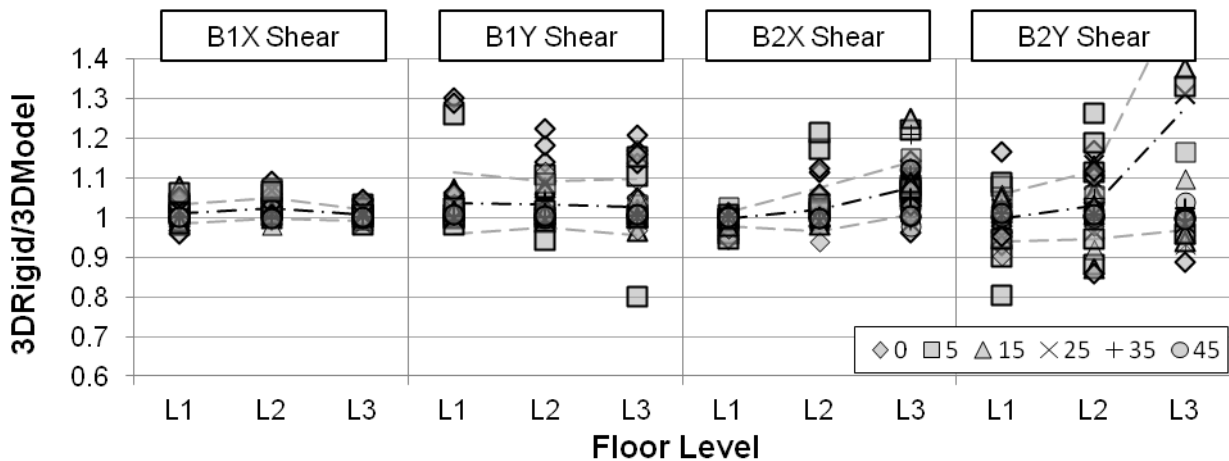

Figure 5.1 Effect of diaphragm flexibility on interstorey shears

Y axis sensitivity is also more pronounced in the beam ductilities (Figure 5.2). In this figure, beam maximum ductilities from Y axis motion, and curvature ductilities are presented (in addition to the X beam ductilities presented in Figure 4.2). Ductilities can be greatly affected by diaphragm rigidity. Building 2's maximum column ductilities are greatly overestimated by 3DRigid. The members with the maximum ductilities recorded in Building 2's columns are located at the four corners of Level 3. When Level 3 is modelled with diaphragm flexibility, much of this load is transferred through the more flexible perimeter columns. When Level 3 is rigid however, more load is directly transferred to the stiffer corner columns which increases the critical building demand. Building 1 does not present a similar trend because its critical column ductilities occur at Level 2, which has much stiffer

diaphragms. The ductility amplifications can be significant for individual records; however, the average results are generally within 10% of the flexible diaphragm results (excluding Building 2's columns). Providing flexible roofs are not being modelled, this suggests that rigid diaphragms would provide suitably agreeable results if averaged ductilities and interstorey shear results from multiple analyses were used.
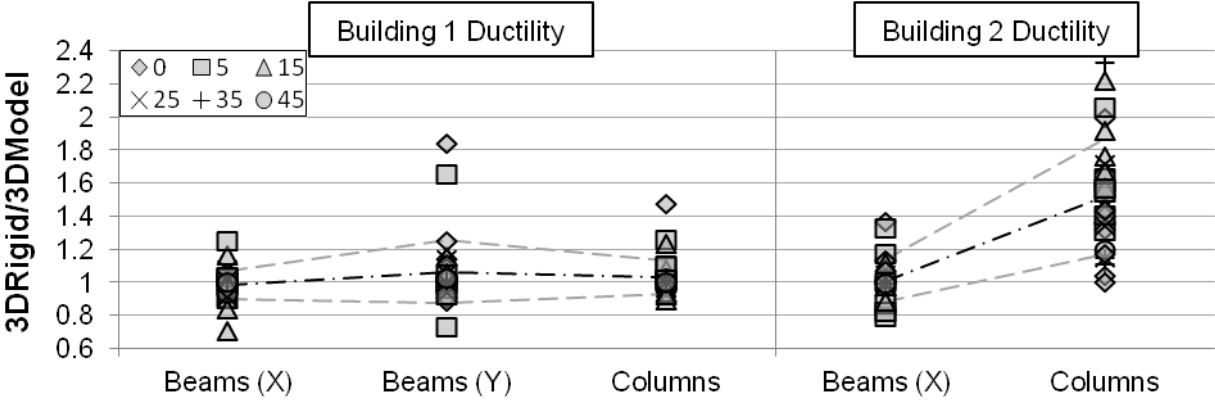

Figure 5.2 Effect of diaphragm flexibility on building ductilities

5.2 Local Damage Changes due to Floor Rigidity

As discussed in previous research (Cole et al. 2011), rigid diaphragms' contact forces are determined by the contact element stiffnesses and do not necessarily reflect the actual force expected during a collision. However, the effect of rigid diaphragms on friction forces is not immediately apparent. Figure 5.3 presents the contact force and friction force amplifications due to diaphragm rigidity at Level 2 and Level 3.
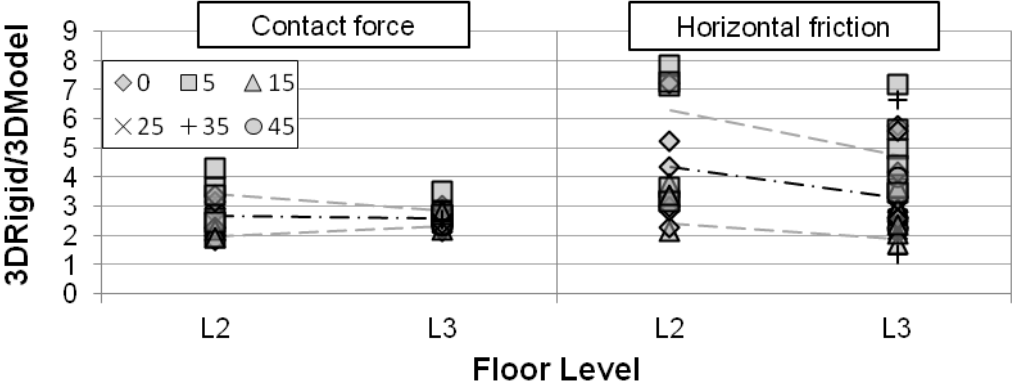

Figure 5.3 Effect of diaphragm flexibility on contact force and friction force

The friction force amplifications are considerably higher than those of the contact force. This is because the total friction force is found by summing the friction forces reported at each contact element. When a flexible diaphragm is modelled, individual contact elements' maximum friction forces occur at different times. However, when rigid diaphragms are modelled, all friction maxima occur simultaneously. In more practical terms, rigid diaphragms overestimate contact friction because they assume complete and immediate participation of both diaphragms' masses. In reality friction load transfer involves a shearing force that travels through each diaphragm as a wave. Friction and contact loads are not well predicted using rigid diaphragms.

6. CONCLUSIONS

Based upon the results presented in this paper, the following conclusions are drawn:

1. Global damage due to pounding generally decreases with increasing building separation

2. Local damage is predominately insensitive to building separation. This could potentially cause considerable damage to building configurations previously thought to be relatively resilient to pounding. Fortunately, such damage is unlikely to be catastrophic.

3. From the limited study presented here, it appears that when buildings are modelled using rigid diaphragms, reasonably accurate global demand results may be obtained by taking the average of multiple (greater than ten) analyses. However, local damage cannot be predicted in this manner.

REFERENCES

Anagnostopoulos, S. A. and Spiliopoulos, K. V. (1992). Investigation of Earthquake Induced Pounding between Adjacent Buildings. *Earthquake Engineering & Structural Dynamics* **21**(4): 289-302.

Carr, A. J. (2007). *Volume 3: User Manual for the 3 Dimensional Version Ruaumoko 3d*. Christchurch, University of Canterbury.

Cole, G., Dhakal, R., Carr, A. and Bull, D. (2011). An Investigation of the Effects of Mass Distribution on Pounding Structures. *Earthquake Engineering & Structural Dynamics* **40**(6): 641-659.

Dong, P. (2003). Effect of Varying Hysteresis Models and Damage Models on Damage Assessment of R/C Structures under Standard Design Level Earthquakes Obtained Using a New Scaling Method. *Civil Engineering*. Christchurch, University of Canterbury. **PhD**.

Fenwick, R. and MacRae, G. (2009). Comparison of New Zealand Standards Used for Seismic Design of Concrete Buildings. *BULLETIN OF THE NEW ZEALAND SOCIETY FOR EARTHQUAKE ENGINEERING* **42**(3): 087-203.

Jankowski, R. (2009). Non-Linear Fem Analysis of Earthquake-Induced Pounding between the Main Building and the Stairway Tower of the Olive View Hospital. *Engineering Structures* **31**(8): 1851-1864.

Jankowski, R. (2012). Non-Linear Fem Analysis of Pounding-Involved Response of Buildings under Non-Uniform Earthquake Excitation. *Engineering Structures* **37**(0): 99-105.

Kramer, S. L. (1996). *Geotechnical Earthquake Engineering*. Upper Saddle River NJ, Prentice Hall.

Lopez-Garcia, D. and Soong, T. T. (2009). Evaluation of Current Criteria in Predicting the Separation Necessary to Prevent Seismic Pounding between Nonlinear Hysteretic Structural Systems. *Engineering Structures* **31**(5): 1217-1229.

Mouzakis, H. P. and Papadrakakis, M. (2004). Three Dimensional Nonlinear Building Pounding with Friction During Earthquakes. *Journal of Earthquake Engineering* **8**(1): 107-132.

NZS1170.5 (2004). Structural Design Actions. *Part 5: Earthquake Actions - New Zealand*. Wellington, Standards New Zealand.

Pallett, P., Gorst, N., Clark, L. and Thomas, D. (2002). Friction Resistance in Temporary Works Materials. *Concrete* **36**(6): 12-12.

Papadrakakis, M., Apostolopoulou, C., Zacharopoulos, A. and Bitzarakis, S. (1996). Three Dimensional Simulation of Structural Pounding During Earthquakes. *Journal of Engineering Mechanics* **122**(5): 423-431.

ULIEGE (2007). Analysis of Hammering Problems. Stage 2. *LessLoss Project: Risk Mitigation for*

Earthquakes and Landslides Integrated Project, Sixth Framework Programme Project No. GOCE-CT-2003-505488, Sub Project 7 - Techniques and methods for vulnerability reduction, LESSLOSS.

Wilson, E. L. and Penzien, J. (1972). Evaluation of Orthogonal Damping Matrices. *International Journal of Numerical Methods in Engineering* **4**: 5-10.

Wolf, J. P. (1994). *Foundation Vibration Analysis Using Simple Physical Models*. Englewood Cliffs, NJ, PTR Prentice Hall.